

# Electron Scattering off Nuclei With Neutron and Proton Excess

Matteo Vorabbi

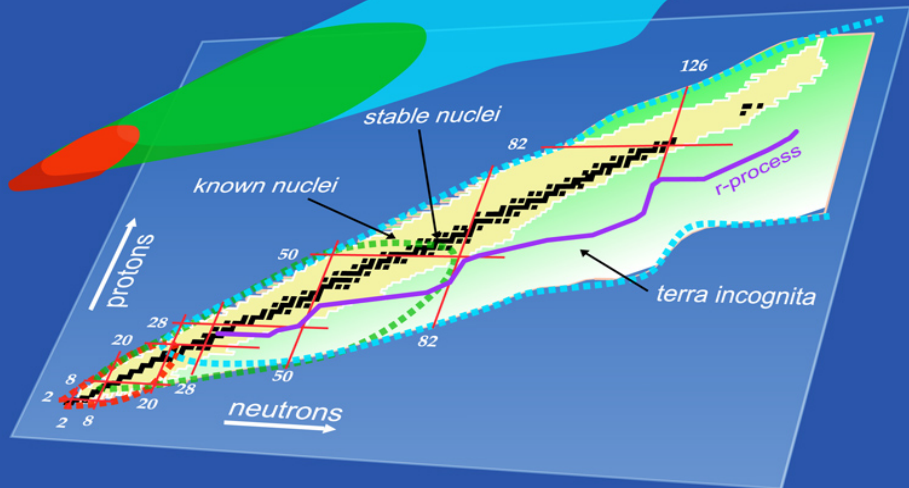
Dipartimento di Fisica - Università di Pavia



Saclay - April 27, 2016

# Nuclear Landscape

- Ab initio
- Configuration Interaction
- Density Functional Theory



# PURPOSE

We study the evolution of the scattering observables for electron scattering on isotopic and isotonic chains

## Isotopes

$$Z = 8 : \quad {}^{14}\text{O} - {}^{28}\text{O}$$

$$Z = 20 : \quad {}^{36}\text{Ca} - {}^{56}\text{Ca}$$

## Isotones

$$N = 14 : \quad {}^{40}\text{Mg} - {}^{56}\text{Ni}$$

$$N = 20 : \quad {}^{28}\text{O} - {}^{46}\text{Fe}$$

$$N = 28 : \quad {}^{22}\text{O} - {}^{34}\text{Ca}$$

Phys. Rev. C **87**, 054620 (2013)

Phys. Rev. C **89**, 034604 (2014)

# WHY ELECTRON SCATTERING?

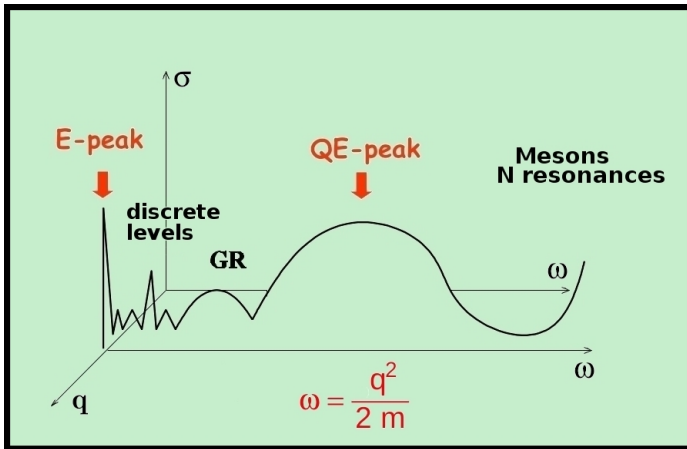
The key element for understanding the structure and dynamics of hadronic matter is its response to an external probe



The electromagnetic probe is the best reliable tool to investigate the nuclear response

1. Validity of the Born approximation
2. Explore the whole target volume
3. The nuclear response can be mapped as a function of its excitation energy

# THE NUCLEAR RESPONSE

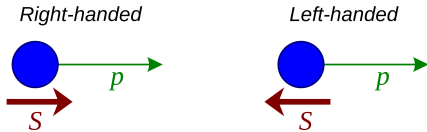


Elastic scattering: global properties  
Quasi-elastic scattering: single-particle properties

# STUDIED PROCESSES

## 1. Elastic scattering

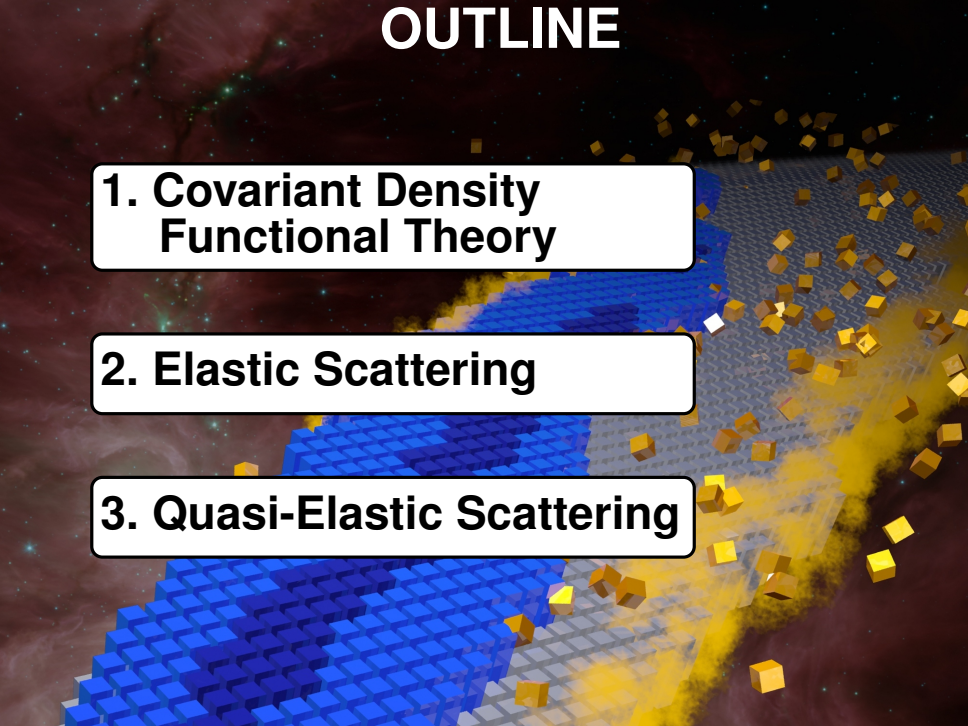
- a) Unpolarized incident electrons
- b) Longitudinally polarized incident electrons



## 2. Inclusive quasi-elastic scattering ( $e, e'$ )

The **width** of the QE peak can give a direct measurement of the average momentum of nucleons in nuclei

# OUTLINE

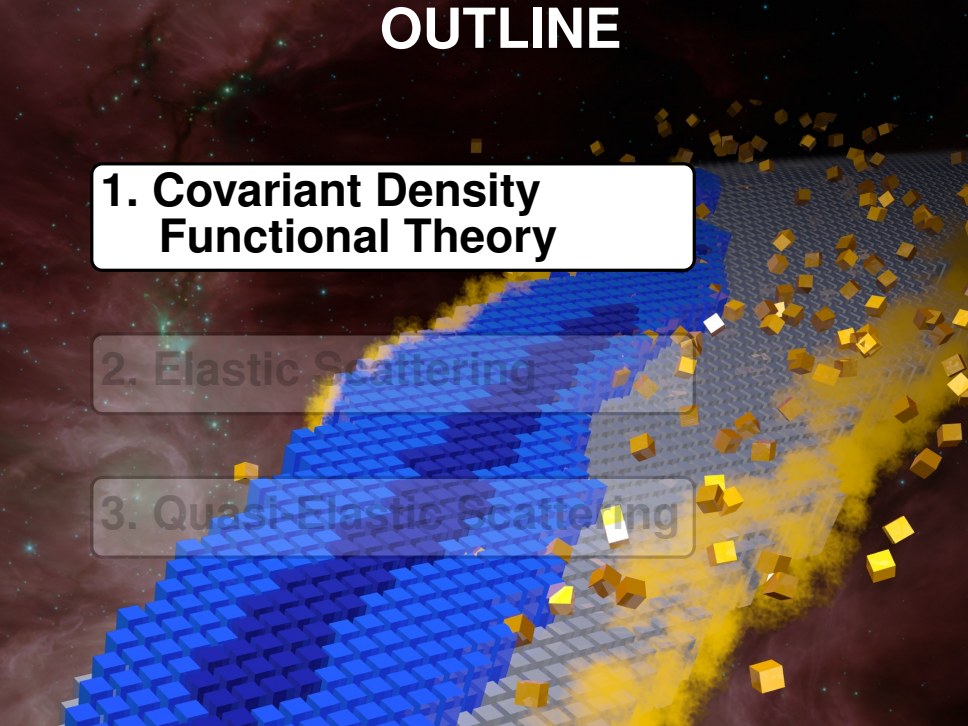
The background features a 3D visualization of a crystal lattice. On the left, a portion of the lattice is composed of blue blocks, while the rest is grey. A bright yellow beam of particles enters from the right, passing through the lattice and scattering particles in various directions. The background is a dark space with faint stars and nebulae.

**1. Covariant Density  
Functional Theory**

**2. Elastic Scattering**

**3. Quasi-Elastic Scattering**

# OUTLINE



**1. Covariant Density  
Functional Theory**

2. Elastic Scattering

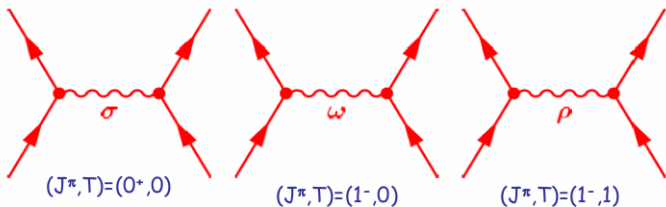
3. Quasi-Elastic Scattering

# COVARIANT DENSITY FUNCTIONAL THEORY

## Quantum Hadrodynamics (QHD)

### Effective theory of nuclear structure

The nucleus is described as a system of Dirac nucleons coupled to the exchange mesons and the electromagnetic field through an effective Lagrangian



$$S(\mathbf{r}) = g_\sigma \sigma(\mathbf{r})$$

Sigma-meson:  
attractive scalar field

$$V(\mathbf{r}) = g_\omega \omega(\mathbf{r}) + g_\rho \vec{\tau} \cdot \vec{\rho}(\mathbf{r}) + eA(\mathbf{r})$$

Omega-meson:  
short-range repulsive

Rho-meson:  
isovector field

# COVARIANT DENSITY FUNCTIONAL THEORY

Relativistic Hartree-Bogoliubov model

$$\begin{pmatrix} \hat{h} - m - \lambda & \hat{\Delta} \\ -\hat{\Delta}^* & -\hat{h} + m + \lambda \end{pmatrix} \begin{pmatrix} U(r) \\ V(r) \end{pmatrix} = E \begin{pmatrix} U(r) \\ V(r) \end{pmatrix}$$

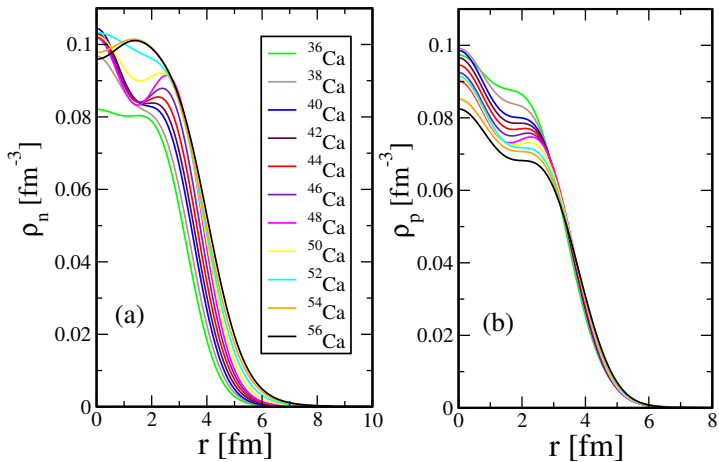


Consistent treatment of mean-field and pairing interactions

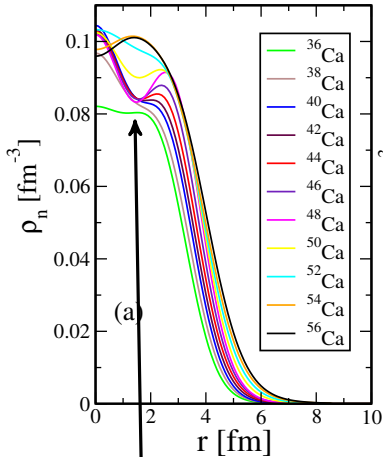
Density-dependent coupling constants

$$g_i(\rho) = g_i(\rho_{\text{sat}}) f_i(x) \quad f_i(x) = a_i \frac{1 + b_i(x + d_i)^2}{1 + c_i(x + d_i)^2} \quad i = \sigma, \omega$$
$$g_\rho(\rho) = g_\rho(\rho_{\text{sat}}) f_\rho(x) \quad f_\rho(x) = \exp[-a_\rho(x - 1)] \quad x = \frac{\rho}{\rho_{\text{sat}}}$$

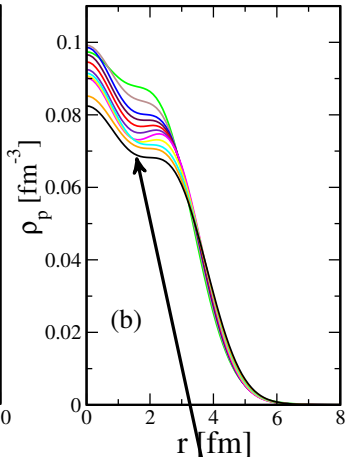
# COVARIANT DENSITY FUNCTIONAL THEORY



# COVARIANT DENSITY FUNCTIONAL THEORY

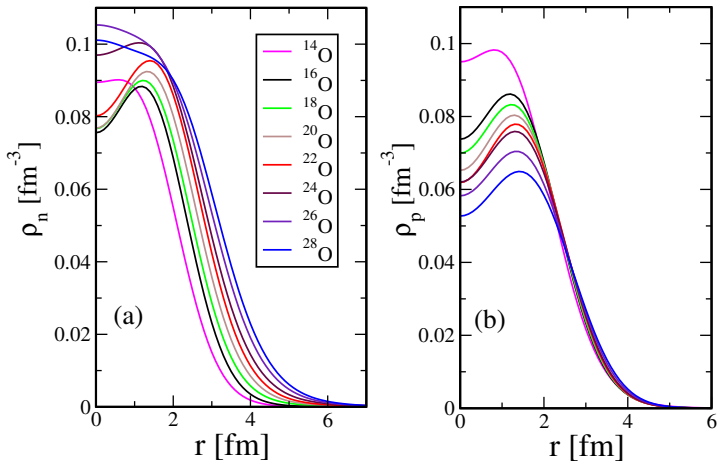


Pronounced shell effects of neutron density profiles in the nuclear interior



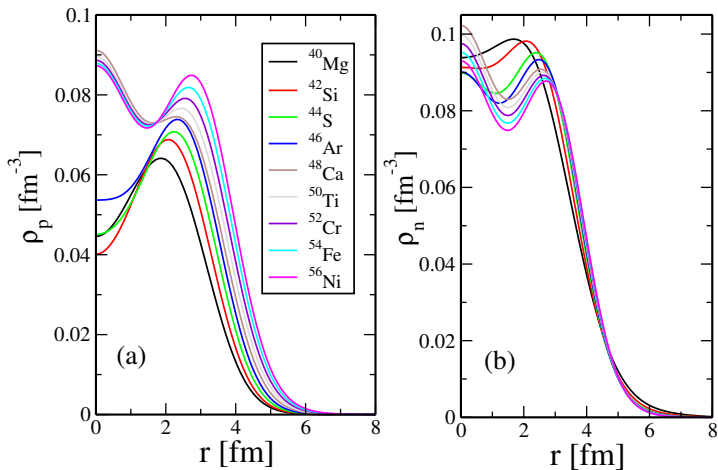
Decrease of proton densities in the nuclear interior

# COVARIANT DENSITY FUNCTIONAL THEORY



Similar results are found  
for the oxygen chain

# COVARIANT DENSITY FUNCTIONAL THEORY



Proton-deficient nuclei

<sup>40</sup>Mg - <sup>46</sup>Ar

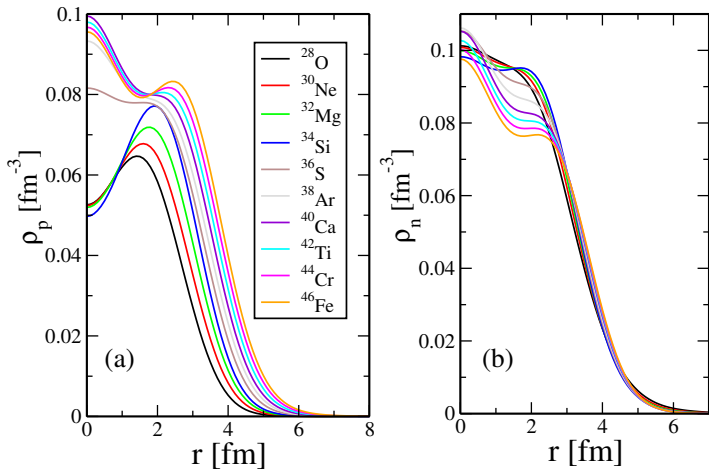
Stable nuclei

<sup>48</sup>Ca - <sup>54</sup>Fe

Proton-rich nucleus

<sup>56</sup>Ni

# COVARIANT DENSITY FUNCTIONAL THEORY



Proton-deficient nuclei

$^{28}\text{O} - ^{34}\text{Si}$

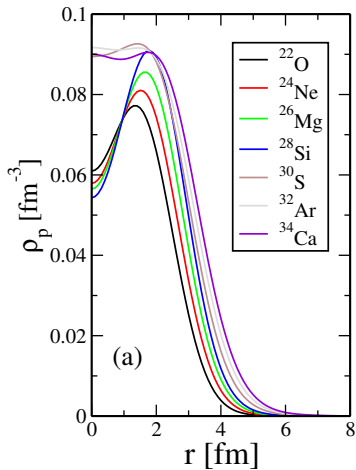
Stable nuclei

$^{36}\text{S} - ^{40}\text{Ca}$

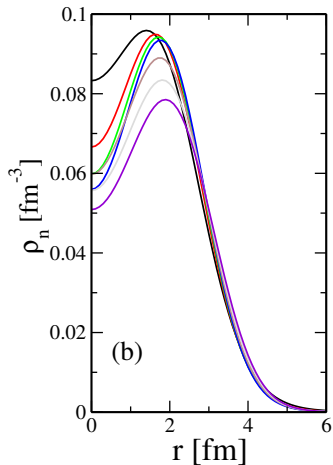
Proton-rich nuclei

$^{42}\text{Ti} - ^{46}\text{Fe}$

# COVARIANT DENSITY FUNCTIONAL THEORY



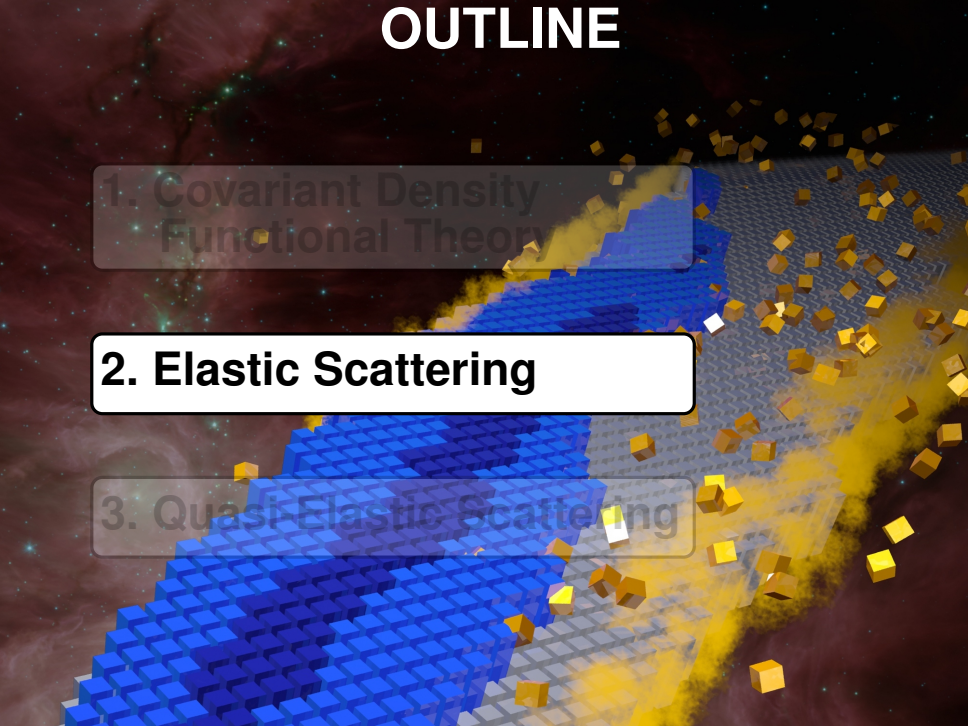
Proton-deficient nuclei  
<sup>22</sup>O - <sup>26</sup>Mg



Stable nucleus  
<sup>28</sup>Si

Proton-rich nuclei  
<sup>30</sup>S - <sup>34</sup>Ca

# OUTLINE



1. Covariant Density  
Functional Theory

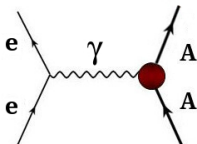
**2. Elastic Scattering**

3. Quasi-Elastic Scattering

# ELASTIC ELECTRON SCATTERING

## PLANE-WAVE BORN APPROXIMATION (PWBA)

### One-photon exchange



The effects of the nuclear Coulomb field on incoming and outgoing electrons are neglected

Differential cross section

$$\frac{d\sigma}{d\Omega} = \sigma_M |F_p(q)|^2$$

Relativistic Mott cross section

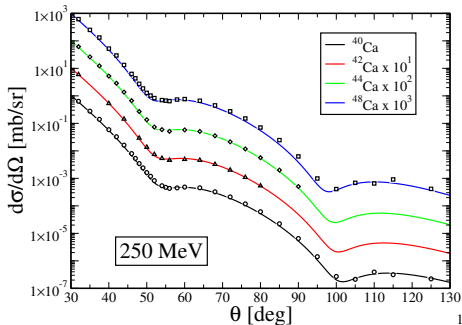
$$\sigma_M(\theta) = \left( \frac{Ze^2}{2E} \right)^2 \frac{\cos^2(\theta/2)}{\sin^4(\theta/2)}$$

Charge form factor

$$F_p(q) = \int d^3r j_0(qr) \rho_{ch}(r)$$

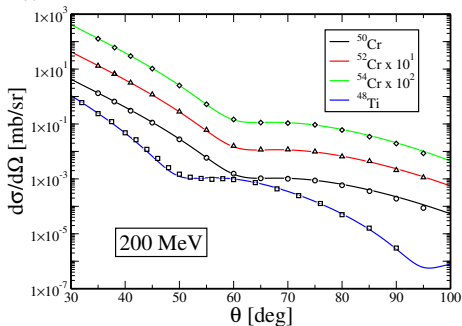
Nuclear charge  
density distribution

# ELASTIC ELECTRON SCATTERING

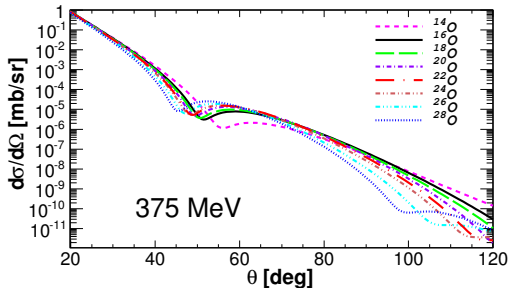


Same behavior as PWBA  
when Coulomb distortion  
is included

Distorted-Wave  
Born Approximation  
(DWBA)

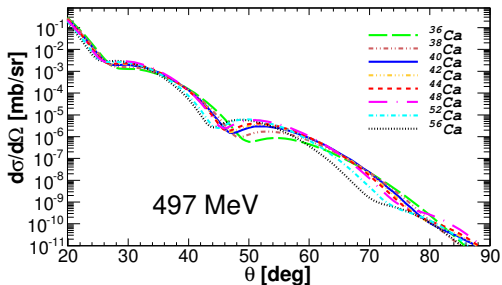


# ELASTIC ELECTRON SCATTERING

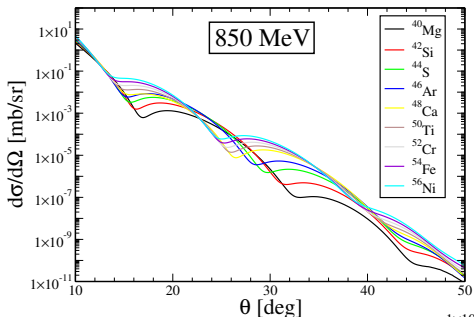


Theoretical results  
for isotopic chains

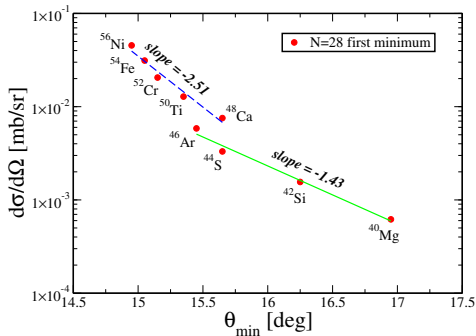
Shift of the minima  
toward smaller angles



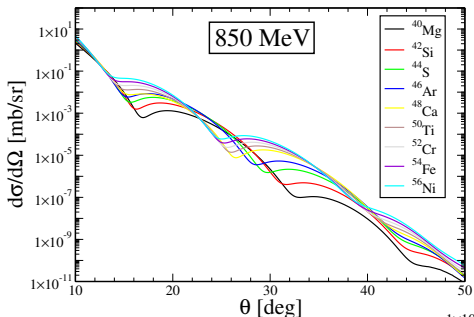
# ELASTIC ELECTRON SCATTERING



Theoretical results  
for N=28 chain

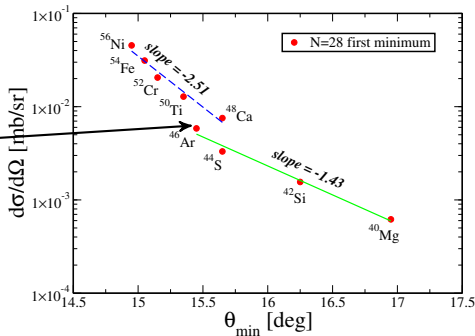


# ELASTIC ELECTRON SCATTERING

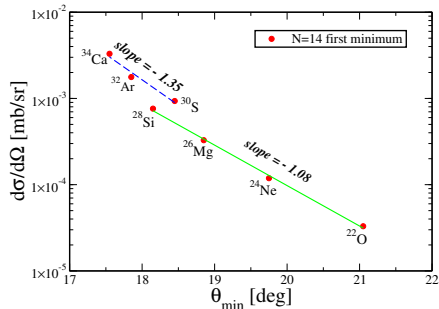
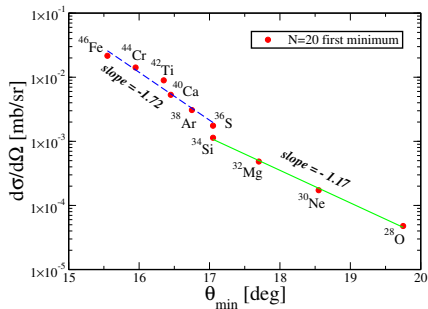
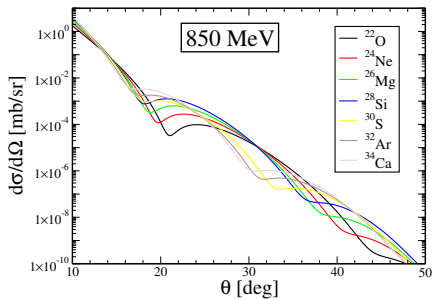
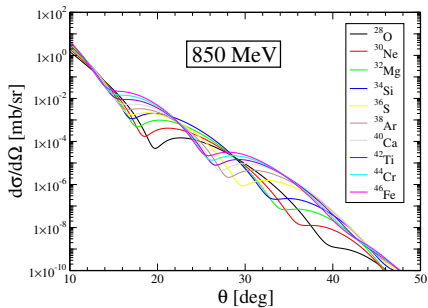


Theoretical results  
for N=28 chain

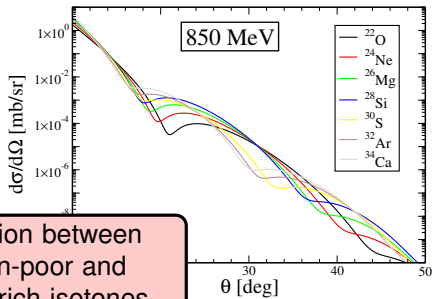
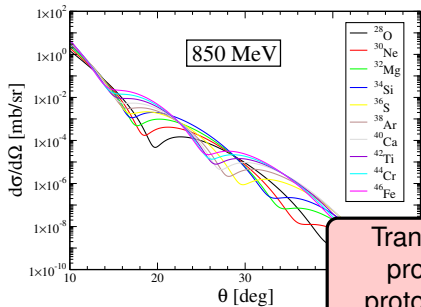
Transition between  
proton-poor and  
proton-rich isotones



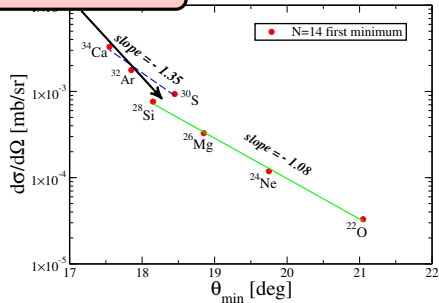
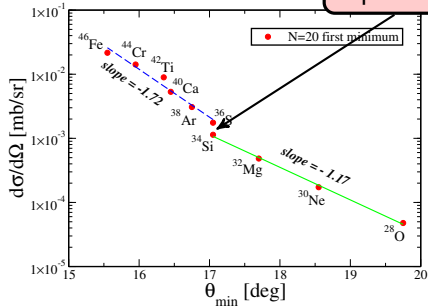
# ELASTIC ELECTRON SCATTERING



# ELASTIC ELECTRON SCATTERING

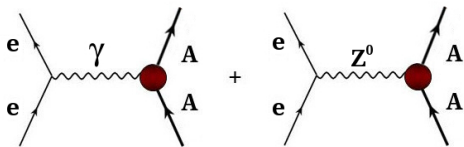


Transition between proton-poor and proton-rich isotones



# PARITY-VIOLATING ELASTIC SCATTERING

One-photon +  $Z^0$ -boson exchange



Elastic scattering between **longitudinally polarized** incoming electrons and a target nucleus

Dirac equation

$$[\boldsymbol{\alpha} \cdot \mathbf{p} + U_{\pm}(r)] \Psi_{\pm} = E \Psi_{\pm}$$

Total potential

$$U(r)_{\pm} = V(r) \pm \gamma_5 A(r)$$

Axial potential

$$A(r) = \frac{G_F}{2\sqrt{2}} \rho_W(r)$$

Weak charge density

$$\rho_W(r) = \int d\mathbf{r}' G_E(|\mathbf{r} - \mathbf{r}'|) \times [-\rho_n(r') + (1 - 4\sin^2\Theta_W)\rho_p(r')]$$

Computation of two different cross sections

$$\frac{d\sigma_-}{d\Omega} : \quad \text{Obtained with left-handed electrons}$$

$$\frac{d\sigma_+}{d\Omega} : \quad \text{Obtained with right-handed electrons}$$

# PARITY-VIOLATING ELASTIC SCATTERING

Parity-violating asymmetry

$$A_{pv} = \frac{\frac{d\sigma_+}{d\Omega} - \frac{d\sigma_-}{d\Omega}}{\frac{d\sigma_+}{d\Omega} + \frac{d\sigma_-}{d\Omega}}$$

Free from uncertainties of strong interactions



Powerful tool to measure the neutron density distribution inside nuclei

Parity-violating asymmetry in Born approximation

$$A_{pv} = \frac{G_F Q^2}{4\sqrt{2} \pi \alpha} \left[ 4 \sin^2 \Theta_W - 1 + \frac{F_n(q)}{F_p(q)} \right]$$

Form factors

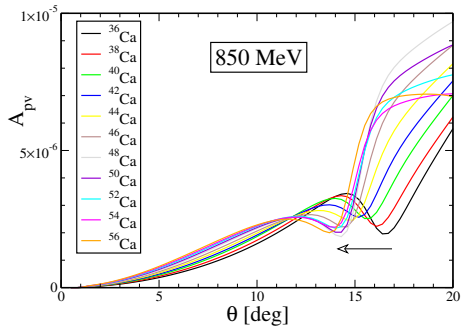
$$F_n(q) = \int d^3r j_0(qr) \rho_n(r)$$

$$F_p(q) = \int d^3r j_0(qr) \rho_p(r)$$

Neutron density distribution inside the nucleus

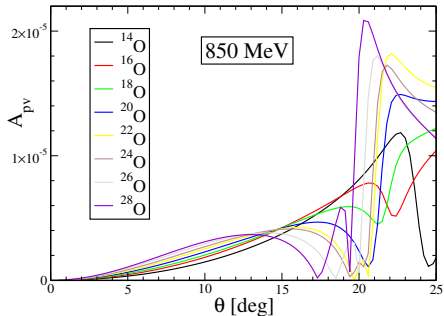
Proton density distribution

# PARITY-VIOLATING ELASTIC SCATTERING



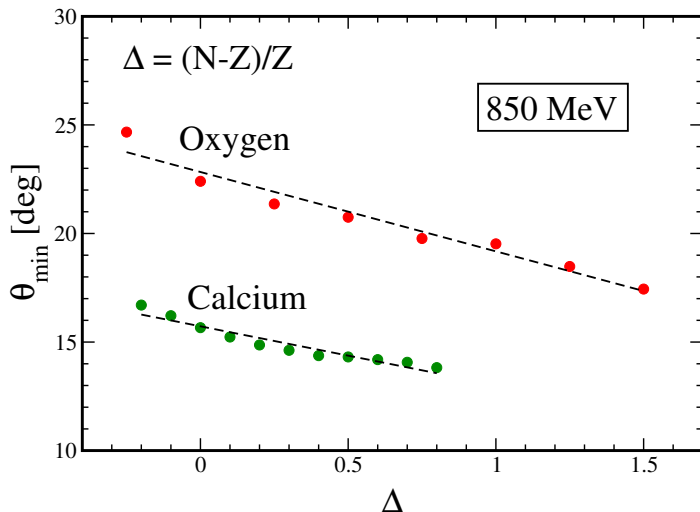
Coulomb distortion effects  
are included

Shift of the minima  
toward smaller angles

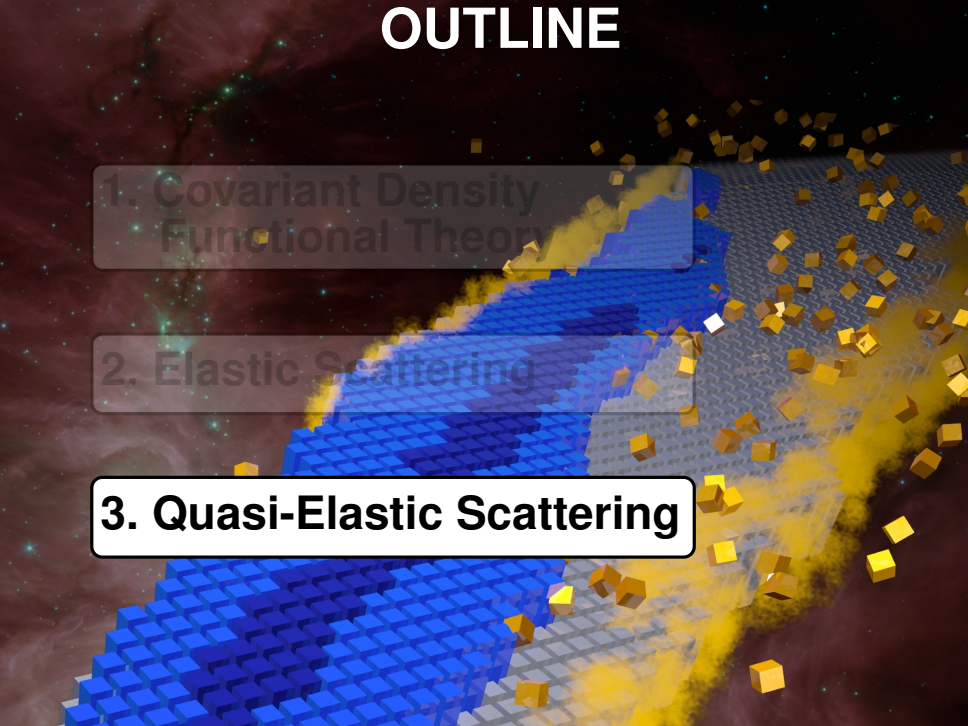


# PARITY-VIOLATING ELASTIC SCATTERING

Linear correlation between  $\theta_{\min}$  of  $A_{pv}$   
and the neutron excess  $\Delta$



# OUTLINE



1. Covariant Density  
Functional Theory

2. Elastic Scattering

**3. Quasi-Elastic Scattering**

# INCLUSIVE QUASI-ELASTIC SCATTERING

Inclusive differential cross section

$$\left( \frac{d\sigma}{d\varepsilon d\Omega} \right)_{QE} = \sigma_M [v_L R_L + v_T R_T]$$

Coefficients

$$v_L = \left( \frac{|Q^2|}{|\mathbf{q}|^2} \right)^2 \quad v_T = \tan^2 \frac{\theta}{2} - \frac{|Q^2|}{2|\mathbf{q}|^2} \quad Q^2 = |\mathbf{q}|^2 - \omega^2$$

Longitudinal and transverse response functions

$$R_L(q, \omega) = W^{00}(q, \omega) \quad R_T(q, \omega) = W^{11}(q, \omega) + W^{22}(q, \omega)$$

Hadron tensor

$$W^{\mu\mu}(q, \omega) = \sum_i \overline{\sum_f} |\langle \Psi_f | \hat{J}^\mu(\mathbf{q}) | \Psi_i \rangle|^2 \delta(E_i + \omega - E_f)$$

# INCLUSIVE QUASI-ELASTIC SCATTERING

## Relativistic Green's function model

Equivalent expression for the hadron tensor

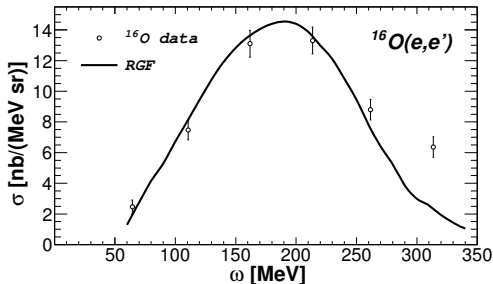
$$W^{\mu\mu}(q, \omega) = -\frac{1}{\pi} \text{Im} \langle \Psi_i | J^{\mu\dagger}(\mathbf{q}) G(E_f) J^\mu(\mathbf{q}) | \Psi_i \rangle$$

Final expression for the hadron tensor

$$W^{\mu\mu}(q, \omega) = \sum_n \left[ \text{Re } T_n^{\mu\mu}(E_f - \varepsilon_n, E_f - \varepsilon_n) - \frac{1}{\pi} \mathcal{P} \int_M^\infty d\mathcal{E} \frac{1}{E_f - \varepsilon_n - \mathcal{E}} \text{Im } T_n^{\mu\mu}(\mathcal{E}, E_f - \varepsilon_n) \right]$$

$$T_n^{\mu\mu}(\mathcal{E}, E) = \lambda_n \langle \varphi_n | j^{\mu\dagger}(\mathbf{q}) \sqrt{1 - \mathcal{V}'(E)} | \tilde{\chi}_{\mathcal{E}}^{(-)}(E) \rangle \\ \times \langle \chi_{\mathcal{E}}^{(-)}(E) | \sqrt{1 - \mathcal{V}'(E)} j^\mu(\mathbf{q}) | \varphi_n \rangle$$

# INCLUSIVE QUASI-ELASTIC SCATTERING



Oxygen kinematics

$$E = 1080 \text{ MeV}$$

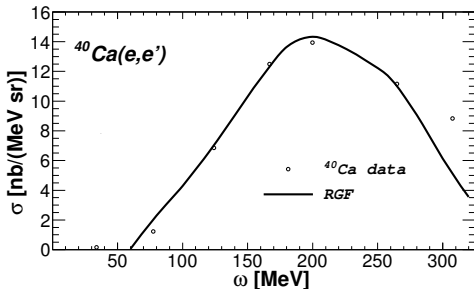
$$\theta = 32^\circ$$

Calcium kinematics

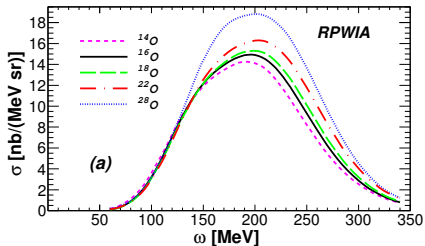
$$E = 841 \text{ MeV}$$

$$\theta = 45.5^\circ$$

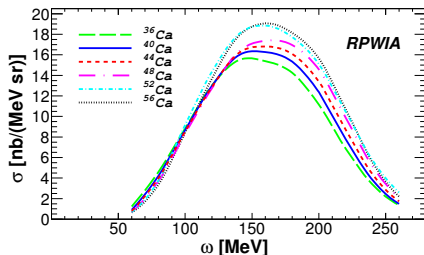
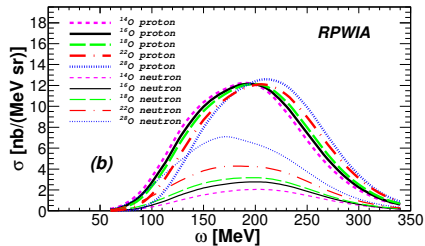
Good agreement with experimental data in the region of the quasi-elastic peak



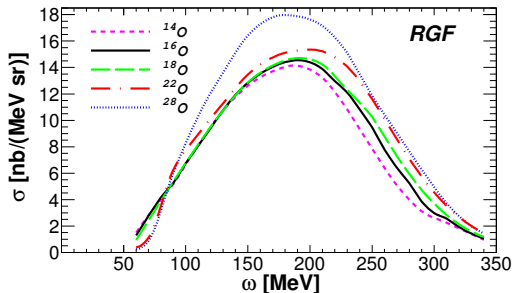
# INCLUSIVE QUASI-ELASTIC SCATTERING



**RPWIA**  
Differences between isotopes are entirely due to single-particle wave functions



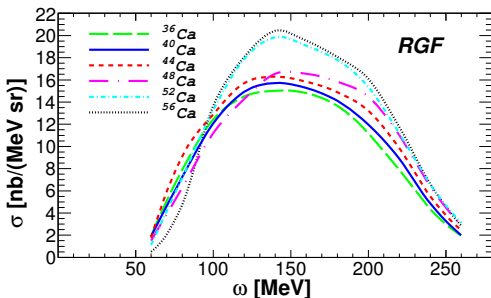
# INCLUSIVE QUASI-ELASTIC SCATTERING



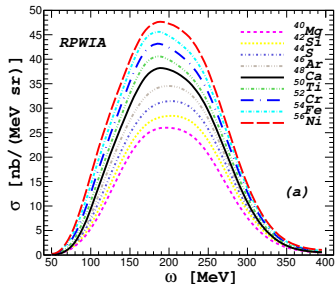
**RGF**

Differences in the low-energy transferred region and in the quasi-elastic peak

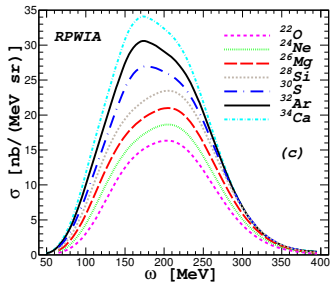
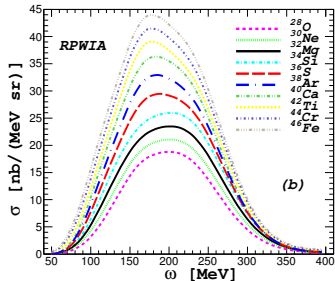
Importance of FSI



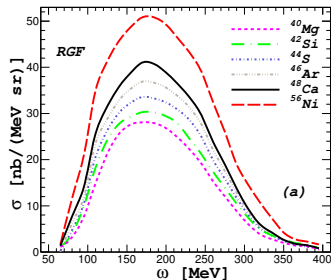
# INCLUSIVE QUASI-ELASTIC SCATTERING



**RPWIA**  
Results for isotonic chains

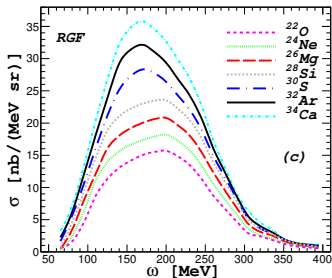
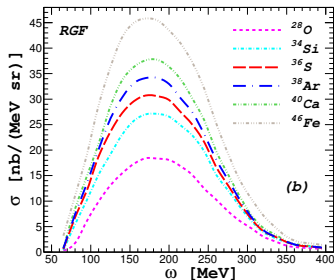


# INCLUSIVE QUASI-ELASTIC SCATTERING

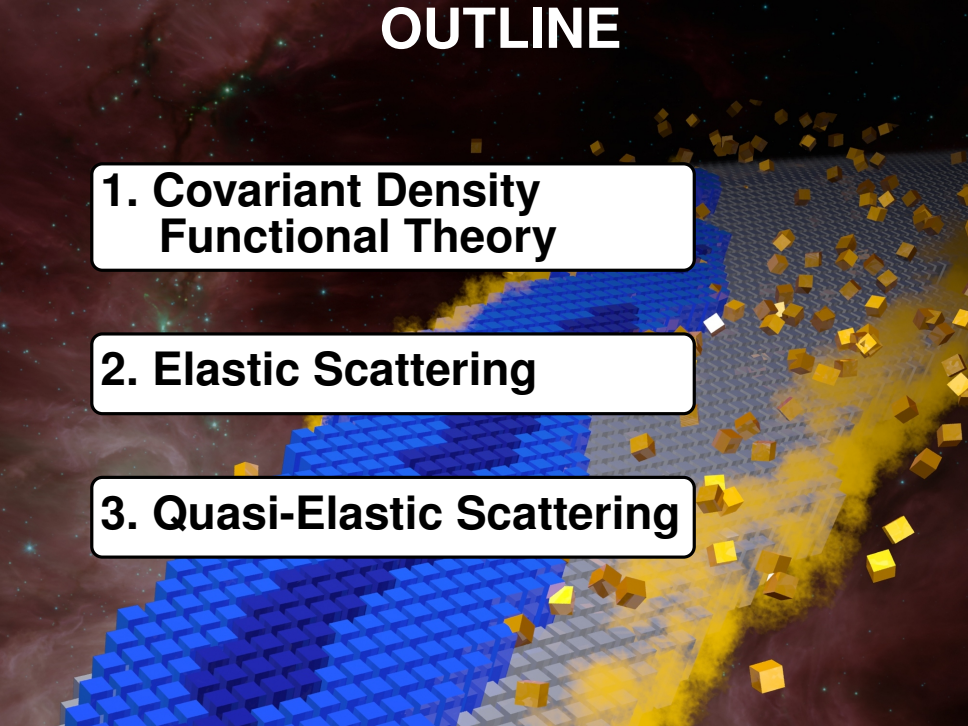


## RGF

1. Visible distortion effects
2. Cross sections show a tail toward large values of the energy transferred



# OUTLINE

The background features a 3D visualization of a crystal lattice. On the left, a portion of the lattice is composed of blue blocks, while the rest is grey. A yellow particle beam, represented by a semi-transparent yellow cylinder, enters from the right and passes through the lattice. Numerous small, yellow, cube-shaped particles are scattered throughout the scene, particularly concentrated around the beam's path and the lattice interface. The background is a dark, starry space with faint nebulae.

**1. Covariant Density  
Functional Theory**

**2. Elastic Scattering**

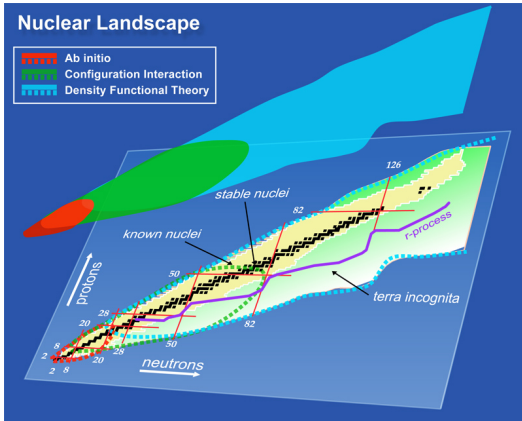
**3. Quasi-Elastic Scattering**

# CONCLUSION

Electron scattering is the best reliable tool to investigate the nuclear properties

1. The interaction is well known and relatively weak
2. Free from most uncertainties of strong interaction
3. Explore the details of inner nuclear structures

# Electron Scattering off Nuclei With Neutron and Proton Excess



1. Covarian Density Functional Theory
2. Elastic Scattering
3. QE Scattering